

Design of a Uni-planar Gy Surface Gradient Coil

R. Lemdiasov¹, R. Ludwig¹, K. Helmer², J. M. Sullivan³, C. Ferris⁴

¹Center for Comparative Neuroimaging, Bioengineering Institute, Worcester Polytechnic Institute, Worcester, MA, United States, ²Biomedical Engineering Department, Worcester, MA, United States, ³Center for Comparative Neuroimaging and Bioengineering Institute, Worcester Polytechnic Institute, Worcester, MA, United States, ⁴Center for Comparative Neuroimaging and Psychiatry department, UMASS Medical School, Worcester, MA, United States

Synopsis

A new design approach and implementation methodology for uniplanar gradient coils for animal studies is presented. The Biot-Savart integral equation is discretized on the basis of numerical inverse formulation. This formulation involves a constraint cost function between the desired field in a particular region in space and the current distribution in the coil plane. The problem can be transformed into a linear matrix equation whose solution yields discrete rectangular current elements with magnitudes and directions within the specified coil plane. The discrete current elements can be synthesized into an overall wire configuration by appropriately combining individual wire loops.

Coil Design Goals

Highly linear and strong magnetic gradient fields enable the high-resolution imaging of biological tissue. The goal of this research is to design a planar surface gradient coil (see Figure 1) that is effective over the typical size of an animal brain. Effectiveness in this context is understood as the ability to provide 1) a strong, and 2) highly linear gradient field within the region of interest (ROI), while concomitantly 3) minimizing the influence of parasitic fields. We introduce a special benchmark criterion

that allows us to capture these three performance requirements and thus enable the comparison of various coil designs: $Q_y = \min_{ROI} \left(|G_y| / \left(G_x^2 + G_y^2 + G_z^2 \right)^{1/2} \right)$ where G_i

($i=x, y, z$) is the z -directed magnetic flux density in the respective coordinate direction. This benchmark has proved to be a useful criterion to assess various surface coil designs. The original G_y surface coil design presented in [1] yields a Q_y of 0.902.

Method

In order to significantly improve upon the existing surface gradient coil designs, we devised a mathematical formulation that determines the optimal current distribution in a given coil plane based on a prescribed field linearity within a given ROI. The coil area is subdivided into a finite number of rectangular elements or current loops. Noticing that only the transversal (or x -axis oriented) component of the current contributes to the longitudinal (or z -axis oriented) magnetic field, we are able to develop a suitable cost function. In addition, current conservation constraints dictate that the sum of the currents flowing in positive and negative x -directions must add up to zero. Casting this in a constrained least-squares formulation, we can solve the resulting system of equations for the optimal current distribution in the coil plane. Figure 2 provides an example for a 6-wire, z -directed, and 4-wire, x -directed, discretization. However, gradient coil implementations by this method are difficult to fabricate, particularly if the current loops are densely discretized in both directions. Guided by our simulations, we can determine the rectangular current flow patterns and diagonally approximate the wire placement along these rectangular patterns. Interestingly, not only does this simplify the coil manufacturing, but it also results in overall higher gradient field strengths. As an example, the coil shown in Figure 3 has four loops, each of which consists of several straight wire paths. To ensure practical realization, the numerical algorithm restricts the number of wires in each loop to fewer than 25. Furthermore, one has to take into account design constraints such as sharp angles and non-overlapping wire paths and loop proximity effects (1 cm minimum in our case).

Coil Performance

To build the coil shown in Figure 3, AWG-20 enameled copper wire was employed. The coil has the following specifications: z and x dimensions are 20x10 cm, ROI is 5x5x4 cm³ and the center is 6cm above the coil plane. The gradient strength in the center of the ROI is $G_y=1.74$ mT/m/A, the inductance is $L=0.49$ mH, and the resistance is $R=1.24$ Ω . Figure 4 demonstrates the amount of image distortion introduced by the coil. It displays how parallel equidistant planes ($y=const$) that are passing through the ROI are distorted. It can be shown that these distortions are significantly less severe than the ones introduced by the previously designed coils [1, 2]. To confirm these results, we inserted the G_y coil in a GE CSI-II 2.0 T 45-cm imaging spectrometer. Images of a phantom consisting of five, 3 mm thick, layers of water separated by Plexiglas plates of the same thickness were acquired (Figure 5). We notice that the distortion pattern is very close to the simulation results seen in Figure 4. The table below summarizes various coil designs [1, 2] and compares them with the coil described in this publication.

Design	G_y [mT/m/A](recorded at height $y=6$ cm)	Q_y (minimum over ROI)
Cho <i>et al.</i> (24 wires maximum)	1.549	0.902
Shi/Ludwig (24 wires maximum)	1.038	0.958
This publication (24 wires maximum)	1.743	0.970

Conclusion

This paper proposes a systematic approach to designing uniplanar surface gradient coils. The current solution to Biot-Savart's integral equation for a desired field distribution yields segmented current elements in terms of magnitude and current direction. The elements can be arranged into individual loops and subsequently combined into surface wire patterns that generate high field strengths and low parasitic fields in a given ROI.

References

- [1] Z. H. Cho and J. H. Yi, J. Magn. Reson., vol. 94, pp. 471-485, 1991.
 [2] F. Shi and R. Ludwig, IEEE Trans. Magn., vol. 32, pp. 195 – 207, 1996

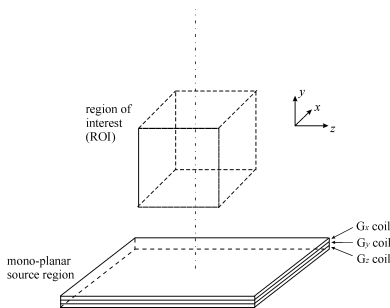


Figure 1: Conceptual arrangement of three mono-planar surface gradient coils situated below ROI.

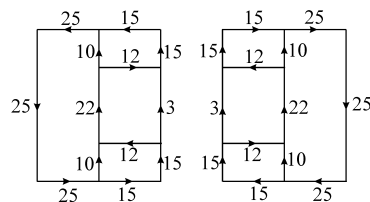


Figure 2: Rectangular G_y -gradient coil.

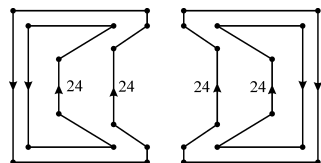


Figure 3: Four-loop G_y -gradient coil.

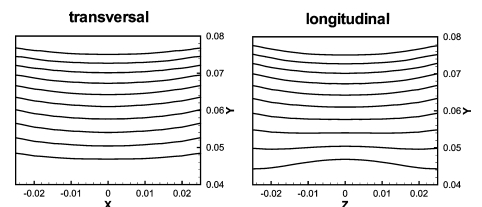


Figure 4: Phantom simulations for transversal (left) and longitudinal image (right) cross sections.

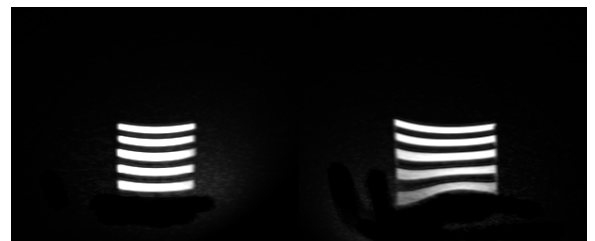


Figure 5: Images of the phantom: transversal slice (left), longitudinal slice (right).